Reverse osmosis fouling mitigation using variable square waves by controlling reject and feed flows based on a distributed control system

Mostefa Ghassoul

Chemical Engineering, College of Engineering, University of Bahrain, Isa Town, Bahrain, email: mghassoul@uob.edu.bh

ABSTRACT

A pseudo-random binary signal (PRBS) type signal superimposed on the operating reject pressure was previously developed to mitigate fouling. The aim was to create a disturbance that results in cleaning the membrane from reversible foulants and hence restoring the membrane near its normal operation. The technique has produced encouraging results. The current paper was an extension of the previous technique where the PRBS was first applied to the reject to confirm the previous results. Then, it was applied to the feed flow, and finally, it was applied to both reject and feed simultaneously but in anti-phase mode. Results have shown that all three techniques have shown a reduction in conductivity and total dissolved salts (TDS). For the flow, the technique has confirmed the previously obtained results when applied to the reject. when applied to the feed only, it did not improve the results significantly. But when applied to the feed and reject, the improvement was quite significant. In fact, the techniques have driven conductivity below 350 μS/cm and TDS below 250 mg/L despite the high temperature. On the flowrate, the third technique has shown a net increase in the flow rate of about 40%. The work was carried out on a lab-scale RO automatically controlled by YOKOGAWA centum VP distributed control system. The mitigation process is automatically triggered when the permeate conductivity hence TDS passes a permissible threshold and/or permeate flowrate is reduced below a certain threshold.

Keywords: Cyclic operation; Fouling mitigation; Reverse osmosis; Reject flow; Feed flow

1. Introduction

With the big increase in human population and desertification of many areas in the world especially in the middle east and sub-Sahara regions, freshwater has become more and more scarce. This requires urgent solutions. Many of them have been proposed. One solution may be applicable on-shore where seawater is in abundance. Other could be implemented in remote areas in humid regions. Extracting water directly from the air would be an immeasurable step forward. But existing technologies generally require high moisture and a lot of electrical energy. This option is expensive and often unavailable. But with emerging solar energy, this could solve the problem. One feasible solution is the use of hydropanels. They collect water vapor from the air, even in areas of low humidity such as arid areas and provide it downstream to tap [1–3]. Unfortunately, this technology needs a huge amount of energy which is quite expensive and may not be available in many areas of need. Luckily, solar energy is coming to the rescue especially with the solar cells cost coming down to a reasonable cost and good solar tracking together with higher solar cell efficiency which is approaching the 50% mark [4,5]. The second visible technique is the extraction of freshwater from seawater. This could be implemented on-shore where seawater is in abundance. On-shore technology uses several techniques to desalt water from the sea such as multi-stage flash distillation (MSF), multi-effect distillation

(MED), vapor compression (VC), and reverse osmosis (RO). RO is probably the most popular due to its simplicity, cost-effectiveness, reliability as well as lower relative energy consumption compared to the thermal processes. Unfortunately, reverse osmosis suffers from major drawbacks, namely, fouling of the membrane. This is exacerbated by concentration polarization. Concentration polarization also results in the reduction of water flux production as well as an increase in the salt content of the product. This contributes to the degradation of the membrane. Fouling not only reduces the permeate flux but also significantly decreases the membrane life. It also increases the energy and feed pressure requirement and increases membrane maintenance and replacement costs. RO fouling could be reduced by adequate pre-treatment steps but cannot be completely removed since it occurs over time. To address this problem, one of the techniques that may be considered is the unsteady-state operation of reverse osmosis. The unsteady operation has been proposed to reduce the concentration polarization effect and generate eddies to clean the membrane surface. One method of unsteady operation is the use of cyclic square pressure waves instead of constant pressure. These square wave pressure pulses generate turbulence and instability at the membrane surface. This helps in reducing the effect of concentration polarization by mixing the water within the concentration polarization boundary layer near the membrane wall. This process enhances the permeate flow rate by reducing the resistance caused by the concentration polarization boundary layer. At the same time, the potential for fouling at the membrane wall is reduced as the foulants that may accumulate at the membrane wall are remixed with the bulk solution. This technique has been implemented by the generation of variable frequency square wave superimposed on the nominal pressure. This wave was applied to the reject flow. The oscillating pressure controls the flow rate through the reject flow [6]. This technique has shown very encouraging results but needs to be investigated further. The current study is an improvement of this technique. Besides generating those variable square wave frequencies, they were applied first to the reject flow only, then to the feed only through a bypass path, and finally to both the reject and feed. The study has shown that applying it to the reject and the feed has produced a better result in terms of flux and salinity as well. Many research and review papers have been published on different ways on how to mitigate and control membrane fouling. One of those techniques is based on chemical treatment (effect of cleaning chemical dose and cross-flow velocity on the membrane chemical cleaning duration to achieve 100% cleaning efficiency (100% [7] and 94.2% [8]). Fouled RO membrane in a pilot-scale desalination system of biologically treated dyeing wastewater containing high chemical oxygen demand (143–228 mg/L) with or without injection of nonoxidizing biocides was presented by Tan et al. [9]. Sodium percarbonate activated with Fe(II) (Fe(II)/SPC) as a feedwater pretreatment strategy for membrane fouling control was addressed by Li et al. [10]. Cross-flow filtration was conducted to investigate RO membrane fouling by concentration mode [11]. A mitigation approach for FO membrane fouling via *in situ* extracting Ca2þ binding with the organic foulants using the gradient diffusion thin-films was

proposed by Li et al. [12]. Boorsma et al. [13] presented a study where they used frequent chemical cleaning to reduce the cleaning frequency. A comprehensive study on the implementation of ultrasound used an external aid to both fouling mitigation control and membrane cleaning was presented by Qasim et al. [14] and Lin et al. [15]. Several review papers on pretreatment were reported. Goh et al. [16] presented membrane development, feed water pretreatment, and membrane cleaning. Lee et al. [17] discussed fouling mitigation in terms of pretreatment, membrane surface modification, and operating conditions for both FO and MD processes. Esfahani et al. [18] introduced a chemical cleaning agent for cleaning fouled spiral-wound RO membrane with sodium alginate solution up to 10% and 15%, respectively at an applied pressure of 1,380 kPa with a flow rate of 10 L/min. Reverse osmosis (RO) desalination system directly integrated with ultrafiltration (UF) pretreatment unit was elaborated by Gao et al. [19]. Guha et al. [20] investigated a nanoparticle-based, *in situ* approach of inducing chemical reaction-based micro-mixing on the membrane surface that can simultaneously eliminate fouling and CP. Computer simulation also had its share in studying membrane fouling where Jiang et al. [21] proposed a spiral-wound RO process model described by differential and algebraic equations with the consideration of membrane fouling. Few papers addressed backwash as a remedy for fouling. (flow reversal to enhance membrane flux in ultrafiltration; periodic reversal of the flow direction of the feed stream at the membrane surface results in prevention and mitigation of membrane fouling presented by Hargrove et al. [22]. Xu et al. [23] discussed an electro-assisted anaerobic forward osmosis membrane bioreactor to treat wastewater and mitigate membrane fouling. Fouling monitoring is critical. Sim et al. [24] reviewed methods to monitor reverse osmosis (RO) membrane fouling, either by characterizing the fouling potential of the feed or by detecting the fouling condition of the membranes. Li et al. [25] used direct current (DC) membrane coupling technology to control membrane fouling, fouling alleviating mechanisms, and membrane filtration performances of the DC electric field membrane coupling process. Al-Bastaki and Abbas [26] reviewed some of the key methods of generating flow instabilities that have been implemented in membrane separation processes during the past few years. The current study is a continuation of a previous study [6]. It concentrates on fouling mitigation online on the membrane by controlling the reject pressure through a pseudo-random binary signal (PRBS) with four different frequencies. Each frequency has a predetermined time window superimposed on the nominal reject pressure. It generates turbulence across the membrane in order to liberate reversible foulant impurities deposited on the membrane so it would be swept away with the reject; hence restoring the membrane to near its normal operation. Though this has given a very promising result, there is still room for improvement. To improve the technique further, besides applying the cyclic signal to the reject pressure only, it was extended and applied to feed pressure alone through a bypass valve. It was then applied in reverse order to both the reject and feed simultaneously. Obtained results have shown that the latter has given very encouraging results. To carry the study further, a comparison study was carried out

by comparing between applying the PRBS on the reject valve alone, then on the feed alone, and finally on both the reject and the feed simultaneously but in reverse order. That means when the pressure on the reject is maximum, it will be minimal on the feed and vice versa. Before applying the technique, the system was modeled. The open-loop transfer function was obtained from a previous study [27]. A positive step test was performed to fit the response to a FOPTD transfer function. A negative step test was performed in order to calculate an average transfer function with a response. The transfer function relating the permeate flow (Q_p) to the reject flow (Q_r) exhibited a negative gain of –0.98445 with a time constant of 0.50555 min and a time-delay of 0.50445 min as shown in Eq. (1):

$$\frac{Q_p}{Q_r} = \frac{-0.98e^{-0.5S}}{0.05S + 1} \tag{1}$$

The objective of the present work is to develop an online mitigation technique to clean the membrane as quickly as possible in order to extend the membrane life and save mitigation time. The technique used in the mitigation is a window of variable frequency square wave superimposed on the nominal pressure simultaneously applied in antiphase to the feed and reject. The mitigation is triggered automatically where the controller monitors both the permeate conductivity and flux. The technique has shown very promising results.

2. System design

The current design is an improvement of a previous design [6] as mentioned earlier in order to improve fouling mitigation. The system is based on a small laboratory scale RO rig with a single FilmTech BW-30-2540 membrane (Fig. 1(8)). Initially, the rig was manually operated where pressure and flow were monitored visually as well as a feed tank (1). The inlet feed flow with a concentration of 2,000 ppm NaCl was pumped to self-cleaning filters (3) by a low-pressure electric pump (2). The filters remove big and organic particles. For the RO to work, water was pressurized. This is done through an electric constant speed pump (4). To apply square wave cyclic pulses, the unit was modified to be fully automated. This section discusses the instrumentation installed and how the unit was interfaced to the distributed control system (DCS) (14) and monitored by the human interface station (HIS) (16). After installation of the required instrumentation, each of the instruments was interfaced to the Yokogawa Centum VP DCS including the DCS hardware such as the input–output (I/O) modules. To achieve accurate control, accurate measurements of the process variables (PVs) are required. The process variables which were desired to be measured were pressures, flow rates, conductivity, total dissolved salts (TDS), and temperature. Control valves were required to manipulate the flows. Two Yokogawa EJA 430A pressure transmitters, one at the inlet of the RO membrane (6), to measure the feed pressure, and one at the reject to measure the reject pressure (11), were installed. The output currents of 4–20 mA analog signals. Two gems FT-110 turbine flow sensors were installed to measure the feed (5)

and reject flow rates (10). The flow sensor output was a frequency output that is too fast to be captured by the DCS. To overcome this problem, an electronic conditioning circuit was designed to convert a 55–550 Hz frequency range delivered by the flowmeter and corresponding to the flow to a current range of 4–20 mA, which could be easily read by the DCS, was designed. Globe control valve (Bruker 2712, Christian Burkert, GmbH & Co. KG, Germany), which is best suited for regulatory control, is installed on the reject line (12). This control valve operates with a pneumatic actuator and digital positioner with an input signal in the range of 4–20 mA. Table 1 shows the equipment installed on the RO process with brief specifications of each. As mentioned earlier, the input pressure pump is of constant speed. It could only deliver a constant flow rate with constant pressure. To implement the new mitigation technique, both feed flow rate and feed pressure have to be controlled. To do so, a new valve (type Burkert 2712) (7) was installed in parallel with the input feed so it could partially or fully divert the flow and reduces the feed pressure. This is shown as valve02 in Fig. 1. To make sure that the mitigation is effective, the temperature is continuously monitored as well as the product conductivity and TDS. Studies have shown that an increase in temperature contributes in increase in product flow [27]. To do so, a MODBUS MEC-10 transmitter was interfaced using MODBUS protocol (15). The transmitter continuously and simultaneously measures the temperature, conductivity as well as concentration. The diverted flow is fed back to the feed (1); the reject is fed to the reject tank (9); and the permeate is fed to permeate tank (13). In order to control and monitor the system, the RO was interfaced to the FCS through appropriate modules. As shown in Fig. 2, the pressure transmitters and flow transmitters were interfaced through the analog input module AAI143-H (channel 04–07), while the bypass and reject control valves were interfaced to an analog output module AAI543-H (channel 01 and 02). Those two modules could either be configured as 4–20 mA loops or as HART modules. For the temperature, conductivity, and TDS, they were read through MEC-10 sensor interfaced to FCS through an RS422/RS485 serial communication module ALR121 configured as a MODBUS protocol. Table 1 shows the DCS modules to which the RO is interfaced.

3. DCS configuration

Programming the DCS is quite delicate and needs special care and this project is no exception. The DCS configuration task is divided into three parts. One is the system configuration and the creation of the faceplates and function blocks. The second is the running of the system in normal mode and the third one is the cyclic cleaning.

3.1. Faceplates

The faceplate is created through a function block called AREAIN to read in the data and allotted a definition parameter %%FT01 for inlet flow, %%FT02 for reject flow, %%PT01 for inlet pressure, %%PT02 for reject pressure, and %%EC for temperature and conductivity. To indirectly measure the product flow and product pressure, an arithmetic CALCU block is called upon. For the parameters

Table 1
RO-DCS configuration

S. No.	Equipment	Model	Short description
(1)	Field Control Station – CPU	AFV30S	Single CP461-10 and power supply – PW482-10
(2)	Analog Input Card	AAI-143H	16-input, isolated – 4–20 mA/HART signal
(3)	Analog output card	AA1-543H	16-output, isolated – 4–20 mA or HART signal
(4)	Digital input card	ADV-151	32 channel, 24 VDC input
(5)	Digital output card	ADV-551	32 channel, 24 VDC, 0.1 A output
(6)	Fieldbus communication card	ALF-111	Foundation fieldbus module
(7)	ProfiBUS card	ALP-111	ProfiBUS communication module
(8)	Serial communication card	ALR-121	RS232/RS485 serial communication module
(9)	Ethernet network card	ALE-111	Ethernet communication module
(10)	Network switches	L2 Switch	Vnet/IP-BUS to connect FCS to ENG or HIS
(11)	HIS/ENG station with yokogawa CENTUM VP® software	Dell Optiplex790	Commercial PC with a network interface card Monitor: DellP190S19" LCD monitor CPU: Intel Core i5, Quad-Core, 3.3 GHz, Ram: 6GB
(12)	Shielded cable for interfacing	Siemens	Shielded installation cable – flexible – 4 Wire
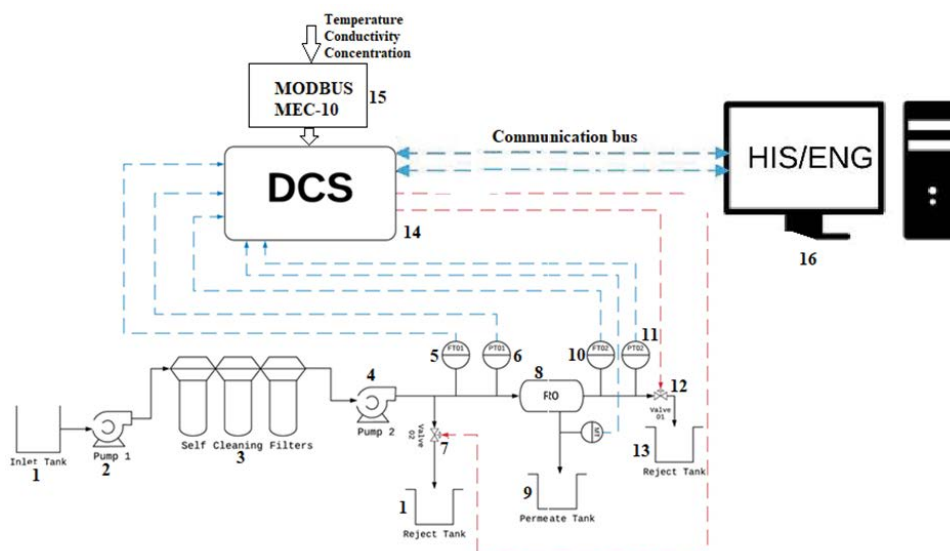
Fig. 1. Schematic of the reverse osmosis process including DCS system.

to be read and displayed on the faceplates, a process variable in (PVI) block is used. To illustrate the point, Fig. 3 shows an example of the faceplate for product temperature (TEMP121). It indicates the status of the function block in the form of a window. The instrument faceplate displays the status and data of a function block, an instrument, or contacts I/O graphically and compactly on a window. The faceplate is not only used for monitoring but for modifying and setting parameters and changing modes by operating the instrument faceplate as well.

3.2. Normal RO operation

The second part of the task is to run the RO system in normal mode using a PID controller to control product flow (FI03) by manipulating the reject control valve

(CONVAL01). Fig. 4 shows the block diagram of the closed-loop. Before implementing the PID controller using the function block, the PID was tuned. In the beginning, the maximum and minimum product flow rates were specified in order to choose the proper set-point to run the system on steady-state, which will be about 50% of the maximum product flow rate. It was found that the maximum flowrate was 4 L/min and the minimum flowrate to be 1 L/min and the setpoint was deduced to be 2 L/min. Then an open-loop test was carried out to find the PID parameters by applying a positive and negative step change on the reject control valve. The results of applying the step change on the MV and CV were modeled using the Ziegler–Nichol tuning method. It was found that $K_c = 0.653$, $\tau_I = 0.7$, and PB = 165.20. The tuning is shown in Fig. 5 and the PID was then implemented as a function block (FC03) as shown in Fig. 6.
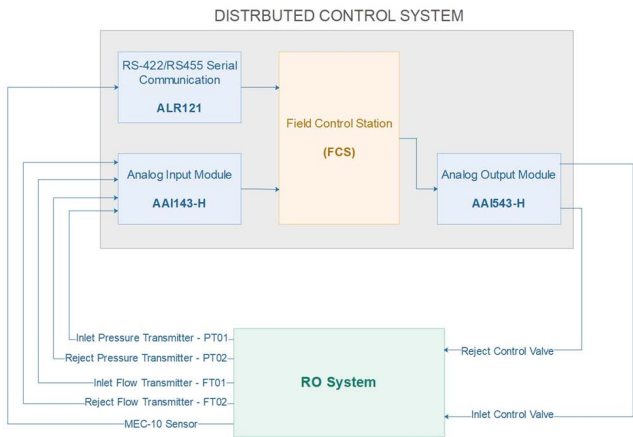
Fig. 2. Interface RO system to DCS.
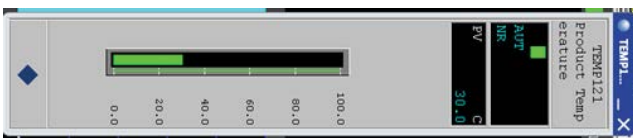
Fig. 3. Product temperature faceplate.
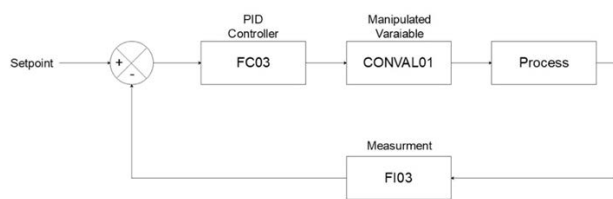
Fig. 4. Closed-loop product flow controller.

3.3. Cyclic cleaning

As mentioned earlier, the cleaning process goes into three steps, applying the step to the reject then applying it to the feed, and finally applying it to both in the reverse order. Before discussing how the cyclic is used, we explain how the cycle is generated.

3.3.1. Frequency generator

The cyclic cleaning is based on four frequency generators based on ON-delay timers each with a different frequency [6]. The ON-delay timer starts running on the leading enable edge. When the time elapses, it sets itself high and stays high until either the enable signal is reset or a reset signal is applied. To obtain the sequence, two timers OND1 and OND2 are used. With the cleaning requirement conditions met, the first-timer OND1 runs for a preset time. When the time elapses, it triggers the second timer OND2. As soon as the second timer starts, it resets the first one and at the same time, it runs for 60 s producing a square wave of 60 s on 60 s off. This sequence runs for 10 min. The next sequence Takes over with OND3 and OND4 and runs for 30 s high, 30 s low for 5 min.

Fig. 5. Product flow tuning window.
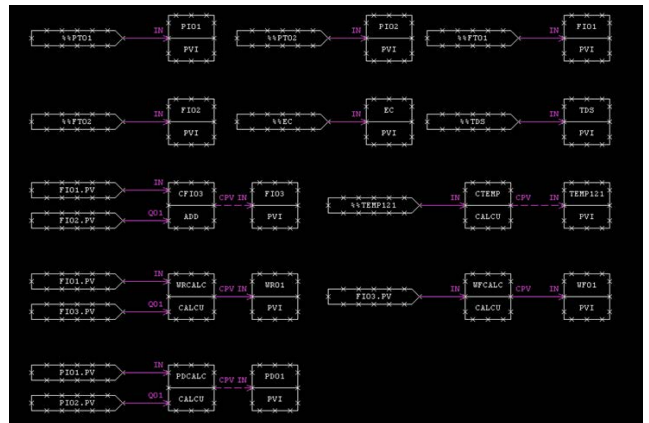
Fig. 6. RO control function block.
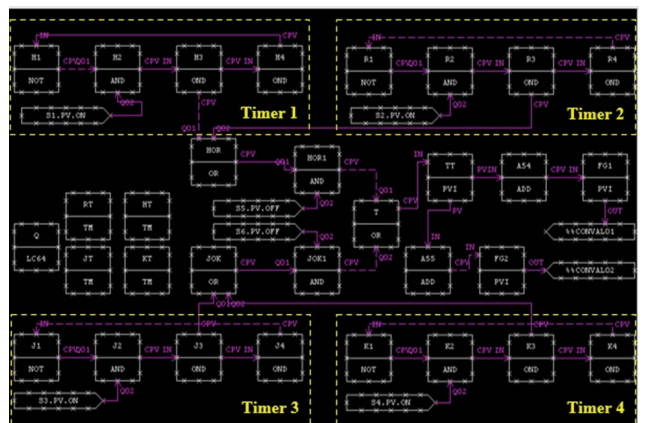
Fig. 7. Sequence generator with different frequencies and periods.

The third sequence takes over for 15 s high–15 s low for another 5 min. Finally, the last sequence takes over for 5 s high–5 s low for another 5 min. Fig. 7 shows how the four frequency generators with the controlling circuitry H, R, J, and K are interconnected. It also shows how those square waves are superimposed on the nominal pressure using the ADD block. It also regulates the sequencing using internal switches S1, S2, S3, S4, S5, and S6. The Q-LC64 sequential
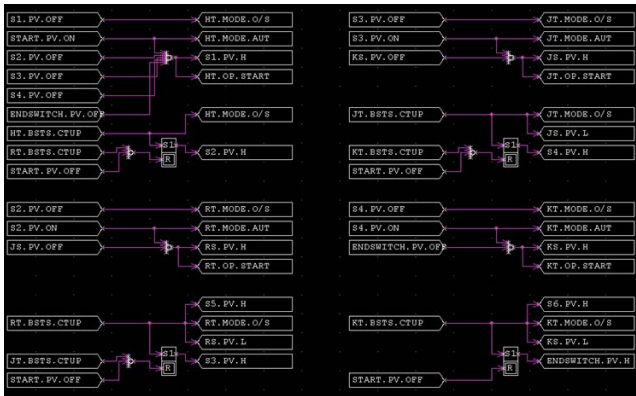
Fig. 8. Logic chart (Q-LC64) sequence frequency generator.
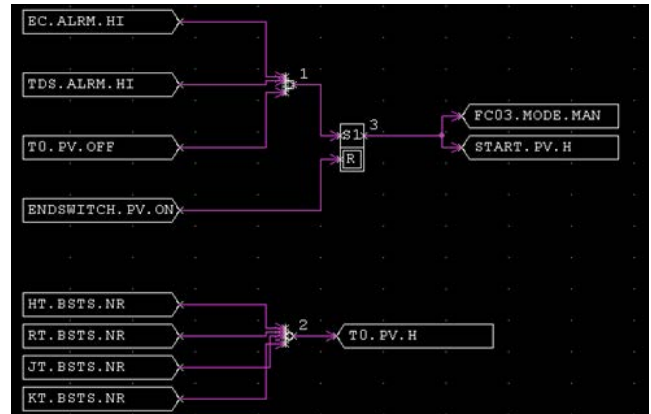
Fig. 10. Automating logic chart.

Fig. 9. Faceplate showing timers and internal switches activation.

block supervises the whole operation. Last but not least, the output signals are applied to both valves through blocks %%CONVAL01 and %%CONVAL02 in inverted form.

3.3.2. Sequence logic chart

When the cleaning condition from high conductivity or/and low flowrate is detected (Fig. 8), it triggers the START soft button in the logic chart (Q-LC64) to start the fouling mitigation process as previously explained; first by activating S1 so H block is turned on. At its cycle end, it is switched out of service (O/S) mode automatically and sets S2 on. Activating S2 starts the second block (RT) hence the second frequency generator as well. Once it ends, the third starts and finally the fourth with the same procedure. At the end of the course, ENDSWITCH will be turned

on. Those changes are demonstrated by the faceplates shown in Fig. 9 where it shows all switches off except S2 on.

Flip-flop (reset–dominant) logic was used to reset the switch when the related block has finished timing.

3.3.3. Automatic cleaning

The aim of the system is to have automatic fouling mitigation. When the conductivity EC and concentration TDS reach a preset threshold, or the product flowrate goes below a preset level, or both conditions are met, the mitigation process is called upon. A logic chart has been developed to set a high limit (HI) for conductivity and TDS and a low limit (LOW) for the product flow rate as well as all the four timers in the off service mode. The automation logic is shown in Fig. 10. When the EC and TDS reach the high limit, the alarm will alert HI. The high limits were set from the tuning window as shown in Fig. 11. When the process variable exceeds PH, the alarm will alert with a high signal (HI), and the same for HH which means very high value. In addition to the high alarms for TDS and EC, all timers are at a halt. When these three conditions are met, the START switch is activated leading to starting the cleaning cycle. Furthermore, an action was designed to set the PID controller in manual mode whenever cleaning is needed. At the end of the cleaning, the start switch is deactivated. A summary of the automatic cyclic cleaning is presented as a flow chart in Fig. 12.

4. Results and discussions

The square wave pressure pulses are superimposed on the nominal pressure to generate limited disturbance and turbulence in the flow along the membrane surface. This turbulence results in mixing the mainstream water with the deposited salt, which reduces the resistance to the permeation of the water through the membrane wall as the concentration at the membrane surface approaches bulk concentration reducing the net driving force. This resistance is caused by the concentration polarization boundary layer, which results in a magnification of the salt concentration near the membrane wall, and hence a magnification of the osmosis pressure. The mitigation

Fig. 11. Electrical conductivity tuning window.
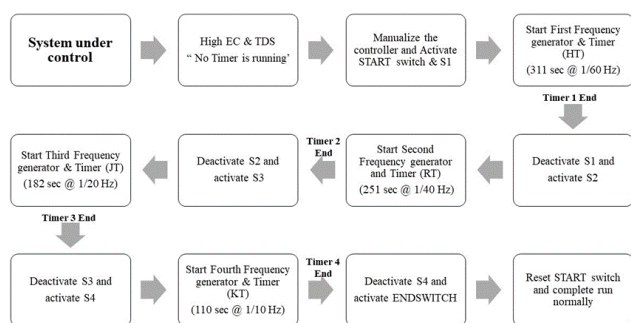
Fig. 12. Procedure of automatic cleaning sequence.

is done by first, applying the cyclic signal to the reject valve only, then applying it to the bypass valve only, and finally, applying it to both the reject and bypass valves but in anti-phase form. That means when reject is minimum, bypass pressure is maximum and when to reject pressure is maximum, the bypass pressure is minimum. This process helps in forcing the fouling impurities to move forward and backward until they dislocate and be rid of with the reject flow. A comparison is then made between the three techniques to deduce which one is more effective. But, before applying for the mitigation course, the system was run in the normal mode under the PID controller.

4.1. Normal run

The product flow was controlled using a PID controller implemented on the reject valve (valve01), to track the setpoint value set at 1.5 L/min while the bypass valve

(valve02) was kept fully closed so there is no bypass of any feed flow (could be considered as disturbance). So, the system was tested as a normally closed-loop control without conducting any kind of cyclic cleaning. As shown in Fig. 13, the PID controller drove the flow until it reached the setpoint value with few oscillations. Therefore, the PID controller tracked the set point in a reasonable time. The same thing could be said about the inlet pressure where it rapidly increased from approximately 270 to 350 psi and stabilized at an acceptable safe range which will supply the membrane to carry out the RO process and protect the membrane from any damages. It is worth mentioning that the increase in pressure at the beginning was due to the increase in the flow to track the setpoint. At the same time, conductivity, TDS, and temperature were monitored. Electrical conductivity (EC) is one of the most important variables to be monitored. As shown in Fig. 14, during the normal run, the EC started above 400 mS/cm, which means that the RO system performed well at the beginning of the normal run. During the process, EC started to increase with the increase of temperature. When the temperature reaches 28°C, the electrical conductivity stabilizes at more than 600 mS/cm, which is a confirmation of a previous study by Rabia et al. [28] on the effect of temperature on electrical conductivity. The TDS was also measured to be more than 250 mg/L. Since it has a direct relationship with electrical conductivity, it can be noticed that it started increasing with the increase of electrical conductivity. Those values show that water is moving in the non-drinkable region. This requires mitigation. So cyclic cleaning has been called upon in order to improve results to move in the region of acceptance by law and chemistry.

4.2. Cyclic operation

Here, we discuss the effect of applying cyclic cleaning on reject valve only, on bypass valve only, and on both valves.

4.2.1. Cyclic cleaning on reject valve

After the normal run, cyclic was applied to the reject valve to clean the membrane while keeping the feed valve fully open by completely closing the bypass valve (valve2). This is shown in Fig. 15a. It shows the four generated cycles:
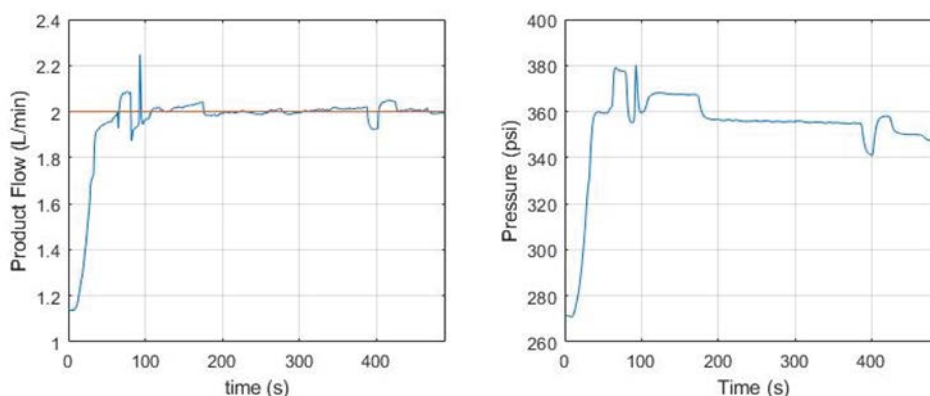
Fig. 13. Product flow and inlet pressure during a normal run.
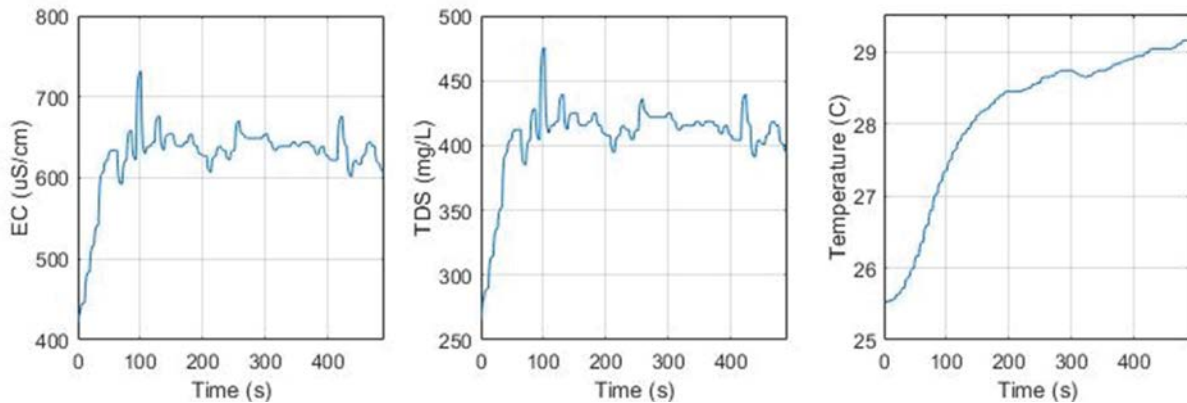
Fig. 14. Conductivity, TDS, and temperature during the normal run.
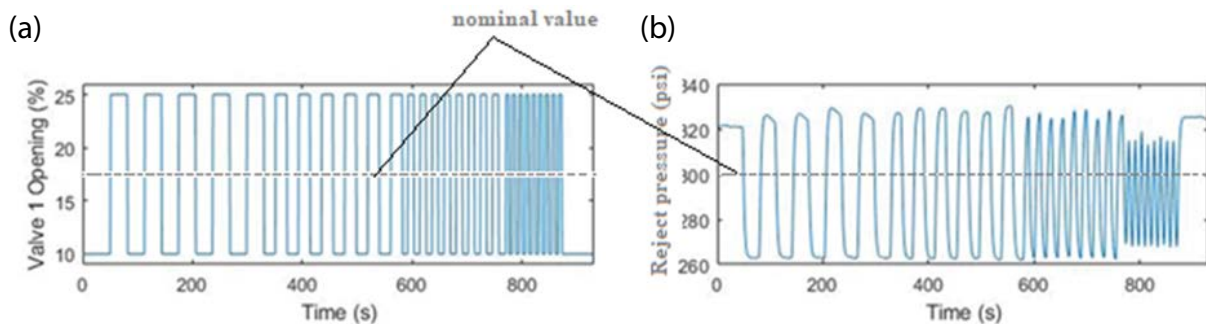
Fig. 15. PRBS applied to reject valve only (valve1) during cyclic1.

60 s high–60 s low for 10 min, then 15 s high–15 s low for 5 min, then 10 s high–10 s low for 5 min, and finally 5 s high–5 s low for another 5 min. In order to open and close the valve for the above course, the valve was automatically programmed to open between 10% and 25%. This variance in valve opening results in inverse variation in reject pressure as shown in Fig. 15b. This in turn creates turbulence on the membrane surface, a type of variable flushing. This tends to dislocate the impurities which will be washed out with the reject flow. It could also be noticed that after certain frequencies, the valve becomes insensitive because it cannot respond fast enough due to its inertia and this explains the filtration of the high frequencies represented by the pulse edges. When the frequency increases more, the valve could not cope further, and this is shown by the reduction of the amplitude of the response. As shown in Fig. 16, electrical conductivity started at about 550 mS/cm and decreased to about 450 mS/cm despite the increase in temperature considerably which tends to increase the conductivity. It is worth mentioning that there is considerable variation during the cyclic. This is caused by the fluctuation of the product flowrate due to the fluctuation of the reject flowrate due to fluctuation of the reject pressure.

4.2.2. Cyclic pulses applied to the bypass valve

Next, the cyclic signal was applied to the bypass valve so that the input flow is controlled. Because the bypass flow oscillates according to the variable PRBS, so does the input flow. At the same time, the reject valve was controlled using the PID controller in order to help in achieving the required product flowrate. As shown in Fig. 17, a sequence of four different frequencies was applied to open and close the bypass valve using the four different timers as explained earlier. As mentioned earlier, the valve toggles between 0% and 23% opening. This effect results in a disturbance in the pressure across the membrane which leads to the release of the impurities on the membrane hence fouling mitigation (Fig. 18). It shows that the technique contributes to reducing the conductivity to 300 mS/cm and TDS to 200 mg/L.

4.2.3. Cyclic pulses applied to both reject valve1 and bypass valve2 in anti-phase

The next step was to apply the anti-phase cyclic pulses to both the reject and bypass valves. That means when valve1 is fully open, valve2 is at its minimum; and when valve1 is at its minimum, valve2 is at its maximum opening. An alternating signal between 10% and 25% superimposed on the nominal value was applied to the reject valve and a reverse alternating signal between 23% and 0% was applied to the bypass valve as shown in Fig. 19. A churn type of agitation is created across the membrane to create a sudden disturbance so as to loosen impurities. Those impurities will be easily washed out with the reject flow. It can also be noticed from Fig. 19, with increasing frequency, the valves could not cope to respond fast enough so the pulse edges tend to be filtered out and the notion of sudden
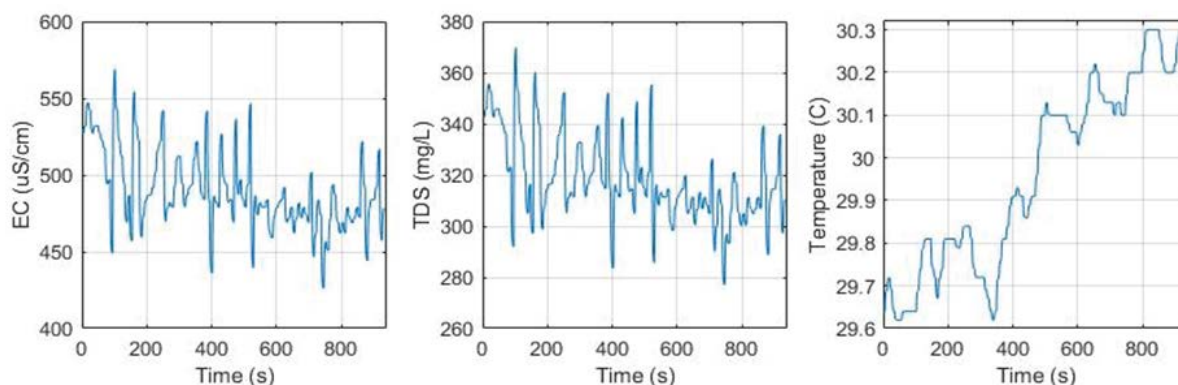
Fig. 16. Process variables during cyclic1.
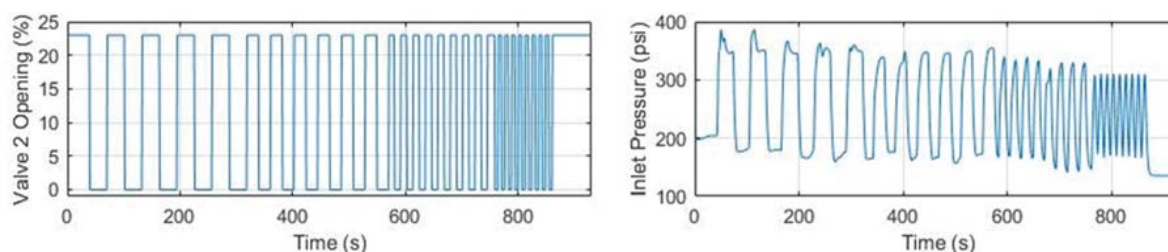
Fig. 17. PRBS applied to bypass valve only (valve2) during cyclic2.
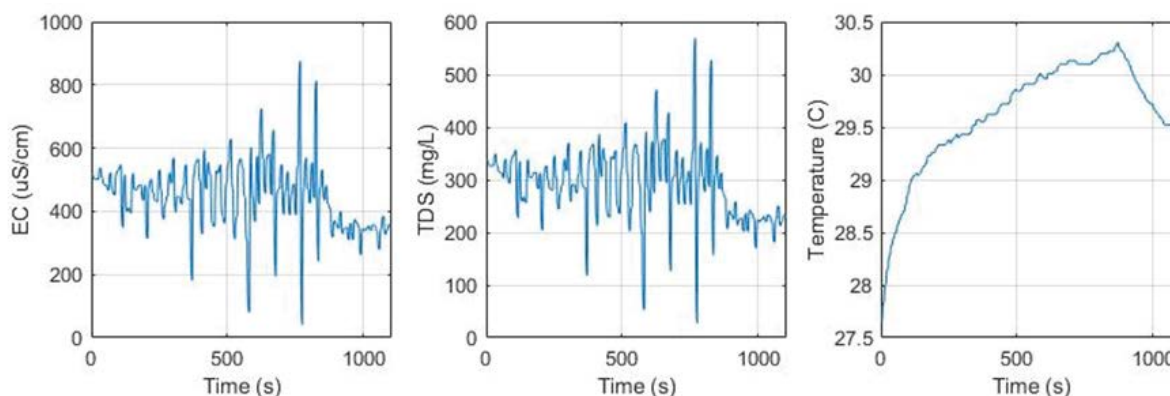
Fig. 18. Decrease of conductivity and TDS during cyclic2.

disturbance is compromised. It is recommended not to drive the valves at high frequencies more than 0.1 Hz. It is shown in Fig. 20 that the electrical conductivity has gone down from 600 to 350 mS/cm and the TDS has gone down from 400 mg/L to around 250 mg/L. which is quite significant.

4.2.4. Three flowrate courses

One of the important aims of fouling mitigation, besides reducing the conductivity and TDS, is the flowrate. The flowrate was monitored continuously and online while the three previous courses were applied. Besides measuring the EC and the TDS as discussed previously, the

online flowrates were measured. The results in Fig. 21, show the three flowrates – cyclic1 – flowrate while controlling only the reject valve – cyclic2 flowrate while controlling only the feed – cyclic3 flowrate while controlling both feed and reject flowrates. During the mitigation process, the flowrate changes according to the valve opening. At the end of the run, application of the course on reject valve only has shown improvement in the flowrate from 1.75 to 1.9 L/min and the permeate flowrate before and after fouling mitigation is shown Fig. 21 cyclic1 and Fig. 22. Whereas applying the course to bypass valve only did not show much improvement (Fig. 21 cyclic2) especially in the improvement of flowrate. Applying the course to both valves has shown a significant improvement where
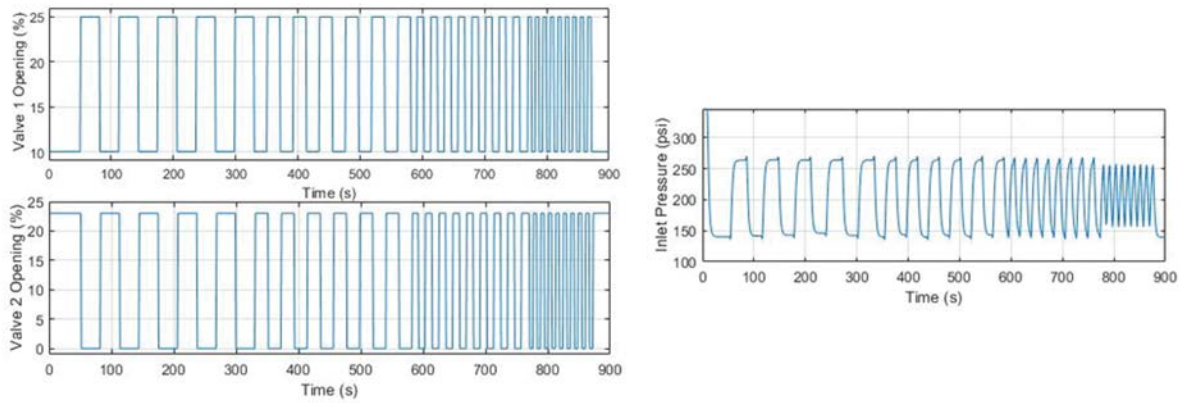
Fig. 19. Valves opening and inlet pressure during cyclic3.
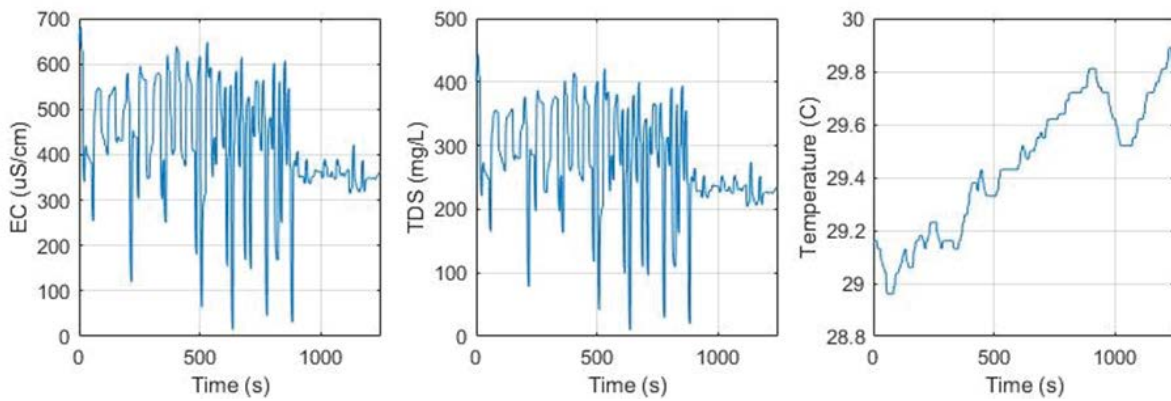
Fig. 20. Conductivity, TDS, and temperature during cyclic3.
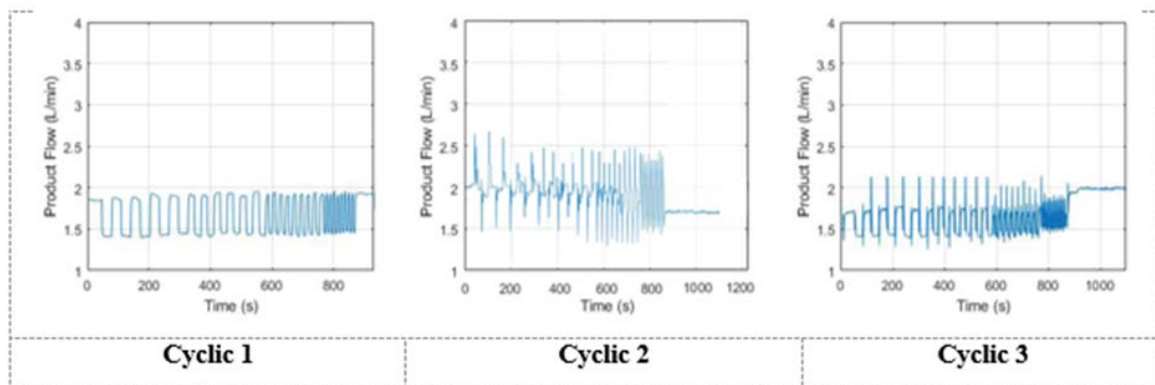
Fig. 21. Product flow rate for cyclic1 (reject control), cyclic2 (only bypass valve controlled), and cyclic3 (both reject and bypass controlled in antiphase).

it has shown an increase from 1.5 to 2.0 L/min. This is a significant increase which is very close to 40% (Fig. 23). The permeate flowrate before and after applying mitigation to both reject and feed valves is shown in Fig. 21 cyclic3. This is a very significant improvement Compared to what was reported in the work, we did previously 28.7% improvement by just applying the cyclic to the reject valve.

4.2.5. Three mitigation scheme using a dose of 4,000 ppm

The membrane used in this work is a small lab scale designed for desalinating brackish water. If a high concentration is used, it may damage the membrane. But even so, a dose of 4,000 ppm was used to test the technique. The results obtained are given in Fig. 24. As it is seen, there is a clear improvement of using the third technique where cycling
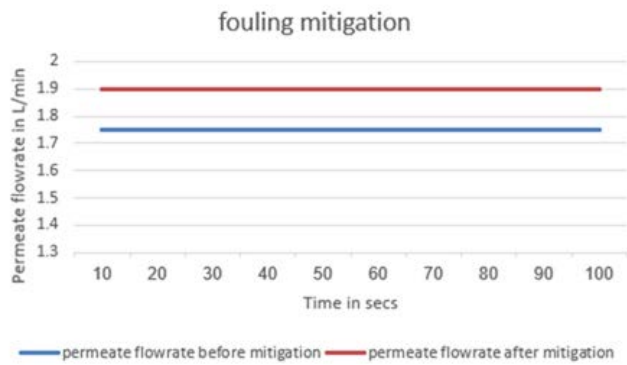
Fig. 22. Flowrate before and after applying mitigation only to reject valve.
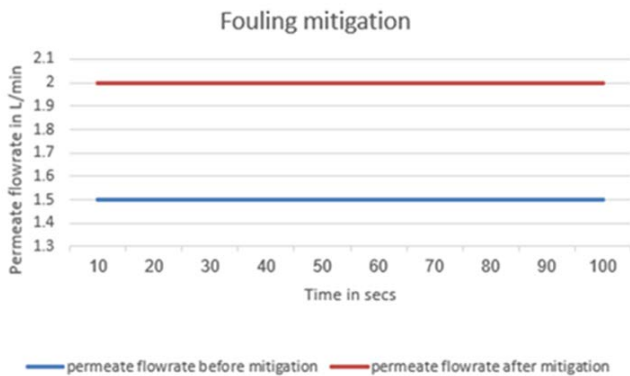
Fig. 23. Permeate flowrate before and after applying mitigation to both reject and bypass valves.

is applied to both reject and feed flows in both reductions of conductivity and increase in flow rate over applying the cyclic to the reject flowrate only or only the feed flowrate only.

5. Conclusion

The study has shown promising results that fouling mitigation could be carried out online without production interruption where it has reduced concentration in polarization hence conductivity and TDS have been reduced to an acceptable level recommended by regulation to less than 350 mS/cm for conductivity and 250 mg/L for the TDS. The study has also shown that the three techniques do contribute to the reduction of the conductivity but it has given contrasting results concerning the flowrate; though applying cyclic to both reject and feed has produced better results. It has also shown that applying mitigation process only to feed flow does not have any significant effect on the flow rate but applying it to reject does contribute to product flowrate going from that though applying mitigating signal only to reject flow produces improvement in product flow rate as well as conductivity and that with accordance with what is reported in the literature to be in the range of 28.7%. Applying mitigation to both reject and bypass valves have produced
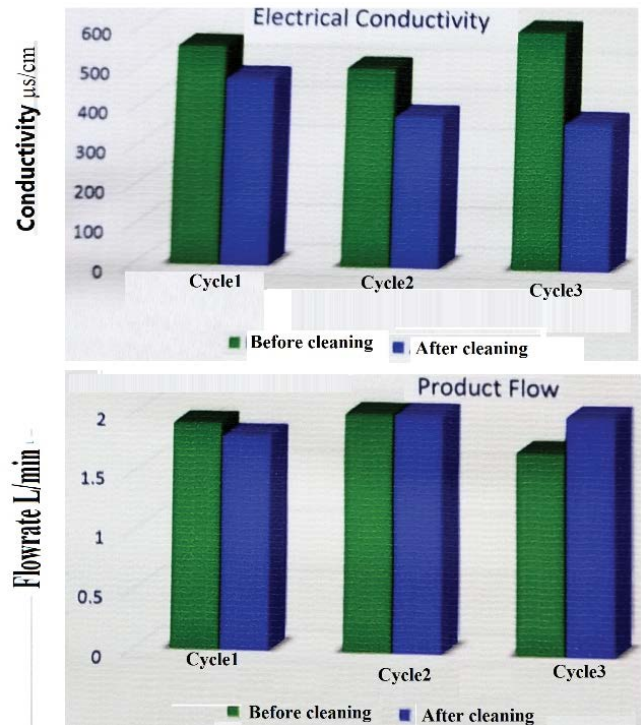
Fig. 24. Conductivity and flowrate for the three-cycle with a concentration of 4,000 ppm.

significant improvement which approaches a 40% increase in flow rate and to an acceptable level in the conductivity as well as TDS. This is no surprise because of the nature of disturbance applied across the membrane. But there is a limit on the mitigation cycle, where any frequency bigger than 5 s high–5 s low (~0.1 Hz) may result in filtering out the edges of the cycle which contribute to generating the disturbance on one side and it may contribute to the shortening of the valve working life. This is due to the slow response of the valves due to their big-time constant.

References

[1] S. Tanavade, S. Manic, A. Al-Khazraji, A. Charkaoui, Water from Sun: An Energy Conservation Initiative for Smart Cities 3rd Smart Cities Symposium, University of Bahrain, 2020, pp. 21–23.
[2] D.J. Nelson, J. Carbeck, Harvesting Clean Water from Air, Public Health E-journal, 2017, pp. 1–28.
[3] N. Fleming, Water from air, New Sci., 243 (2019) 38–41.
[4] M. Ghassoul, Single axis automatic tracking system based on PILOT scheme to control the solar panel to optimize solar energy extraction, Energy Rep., 4 (2018) 1–7.
[5] F. Dimroth, World Record Solar Cell with 44.7% Efficiency, Fraunhoher ISE, September 23, 2013, Press Release 22/13.
[6] M. Ghassoul, N. Al-Bastaki, S. Samsamuddin, Temporary step-wise cyclic operation controlled by DCS to mitigate fouling in RO water desalination, Desal. Water Treat., 168 (2019) 32–41.
[7] V. Singh, A. Das, C. Das, G. Pugazhenthi, M. Srinivas, S. Senthilmurugan, Fouling and cleaning characteristics of reverse osmosis (RO) membranes, J. Chem. Eng. Process Technol., 6 (2015) 1–6.
[8] S.G. Ruiz, J.A.L. Ramírez, M.H. Zerrouk, J.M.Q. Alonso, Optimization of the sequence of washing reverse osmosis membranes used for seawater desalination, Chem. Biochem. Eng. Q., 31 (2017) 21–31.

[9] Y.J. Tan, L.S. Sun, B.T. Li, X.H. Zhao, T. Yu, N. Ikuno, K. Ishii, H. Hong-Ying, Fouling characteristics and fouling control of reverse osmosis membranes for desalination of dyeing wastewater with high chemical oxygen demand, Desalination, 419 (2017) 1–7.

[10] P. Li, X. Cheng, W. Zhou, C. Luo, F. Tan, Z. Ren, L. Zheng, X. Zhu, D. Wu, Application of sodium percarbonate activated with Fe(II) for mitigating ultrafiltration membrane fouling by natural organic matter in drinking water treatment, J. Cleaner Prod., 269 (2020) 1–11, doi: 10.1016/j.jclepro.2020.122228.

[11] Z. Yin, T. Wen, Y. Li, A. Li, C. Long, Pre-ozonation for the mitigation of reverse osmosis (RO) membrane fouling by biopolymer: the roles of Ca2þ and Mg2þ, Water Res., 171 (2020) 1–12.

[12] L. Li, X. Wang, M. Xie, Z. Wang, X. Li, Y. Ren, *In situ* extracting organic-bound calcium: a novel approach to mitigating organic fouling in forward osmosis treating wastewater via gradient diffusion thin-films, Water Res., 156 (2019) 102–109.

[13] M.J. Boorsma, S. Dost, S. Klinkhamer, J.C. Schippers, Monitoring and controlling biofouling in an integrated membrane system, Desal. Water Treat., 31 (2011) 347–353.

[14] M. Qasim, N.N. Darwish, S. Mhiyo, N.A. Darwish, N. Hilal, The use of ultrasound to mitigate membrane fouling in desalination and water treatment, Desalination, 4431 (2018) 143–164.

[15] J.C. Lin, D.J. Lee, C. Huang, Membrane fouling mitigation: membrane cleaning, Sep. Sci. Technol., 45 (2010) 858–872.

[16] P.S. Goh, W.J. Lau, M.H.D. Othman, A.F. Ismail, Membrane fouling in desalination and its mitigation strategies, Desalination, 425 (2018) 130–155.

[17] W.J. Lee, Z.C. Ng, S.K. Hubadillah, P.S. Goh, W.J. Lau, M.H.D. Othman, A.F. Ismail, N. Hilal, Fouling mitigation in forward osmosis and membrane distillation for desalination, Desalination, 480 (2020) 1–23.

[18] I.J. Esfahani, M.J. Kim, C.H. Yun, C.K. Yoo, Proposed new fouling monitoring indices for seawater reverse osmosis to determine the membrane cleaning interval, J. Membr. Sci., 442 (2013) 83–96.

[19] L.X. Gao, A. Rahardianto, H. Gu, P.D. Christofides, Y. Cohen, Novel design and operational control of integrated ultrafiltration — reverse osmosis system with RO concentrate backwash, Desalination, 382 (2016) 43–52.

[20] R. Guha, B. Xiong, M. Geitner, T. Moore, T.K. Wooda, D. Velegol, M. Kumar, Reactive micromixing eliminates fouling and concentration polarization in reverse osmosis membranes, J. Membr. Sci., 542 (2017) 8–17.

[21] A. Jiang, H. Wang, Y. Lin, W. Cheng, J. Wang, A study on optimal schedule of membrane cleaning and replacement for spiral-wound SWRO system, Desalination, 404 (2017) 259–269.

[22] S.C. Hargrove, H. Parthasarathy, S. Ilias, Flux enhancement in cross-flow membrane filtration by flow reversal: a case study on ultrafiltration of BSA, Sep. Sci. Technol., 38 (2003) 12–13.

[23] X. Xu, H. Zhang, T. Gao, Y. Wang, J. Teng, M. Lu, Customized thin and loose cake layer to mitigate membrane fouling in an electro-assisted anaerobic forward osmosis membrane bioreactor (AnOMEBR), Sci. Total Environ., 729 (2020) 1–10.

[24] L.N. Sim, T.H. Chong, A.H. Taheri, S.T.V. Sim, L. Lai, W.B. Krantz, A.G. Fane, A review of fouling indices and monitoring techniques for osmosis, Desalination, 43415 (2018) 169–188.

[25] C. Li, X. Guo, X. Wang, S. Fan, O. Zhou, H. Shao, W. Hu, C. Li, L. Tong, R.R. Kumar, J. Huang, Membrane fouling mitigation by coupling applied electric field in membrane system: configuration, mechanism and performance, Electrochim. Acta, 287 (2018) 124–134.

[26] N. Al-Bastaki, A. Abbas, Use of fluid instabilities to enhance membrane performance: a review, Desalination, 136 (2001) 255–262.

[27] M. Ghassoul, S. Samsamudin, Automating a reverse osmosis process to improve its output yield, J. Eng. Appl., 8 (2020) 8–14.

[28] H.M. Rabia, A.A. Masaad, M.A. Saleh, Automation, Fouling Prediction and Cleaning of a Small Scale RO, and Study of Temperature Effect, Senior Project Report, supervised by M. Ghassoul, Chemical Engineering, College of Engineering, University of Bahrain, 2018.